WILEY | Hindawi

Research Article

Degradation of PVDF-Coated Fabrics after Engineering Applications: Correlations between Surface Microstructure, Physical Properties, and Mechanical Properties Based on Statistical Analysis

Yingying Shang [ID],[1] Bin Yang [ID],[1] Minger Wu,[1] Youji Tao,[2] and Jiaxiang Qin[2]

[1]*College of Civil Engineering, Tongji University, No. 1239, Siping Road, Shanghai 200092, China*
[2]*State Key Laboratory of Environmental Adaptability for Industrial Products, China National Electric Apparatus Research Institute Co., Ltd, Guangzhou 510663, China*

Correspondence should be addressed to Bin Yang; yangbin@tongji.edu.cn

Material degradation has marked impact on the long-term properties and service life of membrane structures. This study is aimed at assessing and understanding the deterioration in visual aspect, surface microstructure, and mechanical properties of a polyvinylidene fluoride (PVDF) polymer after engineering applications. Three groups of PVDF-coated fabrics were removed from different membrane structures in China, which have been used for 15, 16, and 19 years, respectively. Firstly, spectrocolorimetry tests were carried out to determine the evolution of chromaticity and lightness. Other methods such as contact angle and thickness measurements were used to characterize the physical properties. Then, surface morphology was observed by using scanning electron microscope (SEM) technology. Moreover, a series of uniaxial tensile tests and tearing tests were performed to obtain the mechanical indicators including uniaxial tensile strength, strain at break, tearing strength, and uniaxial elastic modulus. In order to further study the degradation mechanism, infrared spectroscopy was used to characterize the molecular structure of aged fabrics. Finally, Principal Component Analysis (PCA) provided a comprehensive description of correlations between surface microstructure, physical properties, and mechanical properties. This paper offers a further understanding of the design, qualification, and durability evaluation of membrane structures.

1. Introduction

In recent years, composites with coating such as polyvinylidene fluoride (PVDF), polyvinyl chloride (PVC), or polypropylene (PP) have been developed rapidly and attracted research interests [1]. Specifically, coated fabrics are increasingly used in civil engineering because of their superiorities such as high strength, light weight, and commercial efficiency. Various kinds of fabrics are prevailingly used as roofing materials for sports halls, shopping malls, and exhibition centres. Since coated fabrics are directly exposed to atmospheric environment during the service period, their properties are distinctly affected by snow, rain, solar radiation,

temperature change, and so on. The degradation mechanism of composites should be studied to guide the structure design. The elaboration of correlations between the physical and mechanical properties during deterioration is helpful to assess material durability.

The mechanical properties and failure process of unaged polymers are investigated by experimental characterization and multiscale modelling in several references [2–8]. Prateek et al. [9] presented a comprehensive review of the use of polymers, especially PVDF and PVDF-based copolymers/blends as potential components in nanocomposite materials for capacitor applications. Rydzkowski et al. [10] manufactured and evaluated the mechanical, morphological, and

thermal properties of reduced graphene oxide-reinforced expanded polystyrene (EPS) nanocomposites. However, researches concerning degradation follow empirical acceler-ated ageing tests, in most instances. The effect of ageing con-ditions and alkali treatment on the mechanical properties of jute reinforced polyester composites was investigated by Albuquerque et al. [11]. Guermazi et al. [12] focused their research on the durability of fibre-reinforced plastic (FRP) composite materials for aircraft structure parts in a hygro-thermal environment. Barbosa et al. [13] studied the influ-ence of artificial accelerated ageing on carbon fibre/epoxy composites. However, accelerated ageing tests are deficient to simulate all the effects of weathering, and results some-times fail to correlate with long-term outdoor exposures. Thakur et al. [14] classified different types of lignin-reinforced polymer composites starting from synthetic to biodegradable polymer matrices and highlighted recent advances in multifunctional applications of lignin.

Field ageing tests which get experimental specimens from real engineering structures can reflect the material deg-radation more accurately. Nevertheless, the field ageing test cycle is excessively long and the acquisition of test specimens is relatively difficult. So there are few published research papers about this type of ageing tests. Zerdzicki et al. [15] have taken the PVC fabric VALMEX from the hanging roof of the Forest Opera in Poland which has been used for 20 years, carried out laboratory tests, and used the Bodner-Partom constitutive equations for modelling. Some scholars have also done researches about naturally aged composites [16–18]. Yang et al. [19] accumulated statistical data of nat-urally aged PVDF-coated fabrics' mechanical properties and calculated structural reliability indexes, to study the durabil-ity of membrane materials. Jakubowicz [20] implemented a natural weathering program in Sweden which underwent 12 years for several kinds of PVC fabrics. However, no obvi-ous relationship was discovered between the results of the artificial and natural ageing tests. Sousa et al. [21] presented both experimental researches and numerical analysis about the durability of adhesively bonded joints, which were made of glass fibre-reinforced polymers (GFRP). It has been noted that for many artificial or natural ageing experiments, the sample size was too small to be statistically significant.

Nowadays, some references have investigated the mechanical properties of aged polymers, relatively more for glass fibre or nature fibre composites, but few for polyester fibre composites. Besides, many scholars concentrated on the degradation of mechanical properties, whereas ignoring the analysis of surface microstructure, the evolution of phys-ical properties, and the relationships among these properties. As a matter of fact, relationships do exist between the visual aspect, microstructure, physical properties, and mechanical properties of polymers [22–24]. Martin et al. [25, 26] studied photodegradation of certain polymers and presented a band theory model to explain reciprocity experimental phenom-ena. Fabiyi et al. [27] verified correlations between lightness evolutions and chemical structure variations of wood plastic composites over long-term weathering. Among these factors of degradation, lightness could be a direct affecting indicator and used to evaluate the changes. As for coated fabrics, rela-tionships between surface microstructure, physical proper-ties, and mechanical properties after engineering applications have rarely been studied. Besides, the relation-ship between these properties was evaluated by pair in previ-ous studies, not all of them simultaneously. To study the correlations between factors in a high-dimensional dataset at the same time, Principal Component Analysis (PCA) is an effective statistical method. By reducing the dimension of high-dimensional data, the main feature components of data are extracted and the relationship between pairs of data can be obtained. In engineering applications of PVDF-coated fabrics, mechanical properties are always the focal point for structural design. Mechanical properties of mem-brane materials are important factors to ensure the accuracy of the design, analysis, and evaluation of membrane struc-tures. Thus, the aim of this study is to find the correlations of surface microstructure with mechanical properties and the correlations of physical properties with mechanical properties.

As an engineering material, coated fabrics are always directly exposed to the natural environment. The degrada-tion behaviours of these materials can be regarded as the cumulative effect of various factors, such as prestress state, external loads, and weather variations. This paper mainly focuses on the performance of aged PVDF-coated fabrics named Précontraint 1202T and emphasizes the relationships between measured properties. Three groups of fabrics were removed from different engineering structures in China, which have been aged for 15, 16, and 19 years, respectively. First, surface aspects were analysed by optical measure-ments; meanwhile, contact angle and thickness measure-ments were also used to characterize the physical properties. Moreover, the degradation of coatings was tested with a scanning electron microscope (SEM) to observe the surface morphology. Infrared spectroscopy technique was applied to characterize the molecular structure. Then, a series of mechanical experiments were performed, including uniaxial tensile tests and tearing tests. The quantity of repli-cates for each test is 40 to reduce statistical limitations, mak-ing the results more accurate. Finally, the PCA method was used to determine the relationships between surface micro-structure, physical properties, and mechanical properties.

2. Materials and Methodology

2.1. Materials. Polyester fabrics named Précontraint® 1202T were taken as the research object in this paper. They were produced by Serge Ferrari, a French company. The fabrics are made of two orthogonal polyester yarns (the warp and weft direction), both surface sides coated with PVDF layers. By applying tensile force to both directions of fabrics, the Précontraint technology is used to obtain more consistent warp and weft stiffness [2, 3, 28]. According to the manufac-ture, the thickness of unaged fabrics is 0.78 mm and the weight is 1050 g/m^2. Three groups of aged fabrics were removed from membrane structures in China, which under-went coupled weathering and mechanical ageing. These materials have been used as the covering of membrane struc-tures in Zhengzhou, Hangzhou, and Nanjing, with ageing

time of 15 years, 16 years, and 19 years, respectively. Meanwhile, one group of unaged fabrics was taken as the control experimental group for contrast. Detailed information about tested fabrics can be found in Table 1.

2.2. Experiment Schematic.

Coated fabrics are widely regarded as orthotropy, which means mechanical properties along two directions are not identical. Therefore, the specimens for mechanical experiments were cut separately along both directions. In the initial tests, it was found that even for the same group of aged fabrics, the mechanical property data were of high discreteness. In order to consider the stochastic characteristic and study the correlation between material properties, 40 specimens were taken along both directions in each group.

Each specimen measuring 300 mm × 150 mm were cut from the fabrics and prepared for different tests. The investigation started with visual property measurements, including spectrocolorimetry characterization, infrared spectrum analysis, contact angle measurements, and thickness measurements. After that, SEM and infrared spectroscopy techniques were performed to analyse the microstructure of the surface coating. Finally, uniaxial tensile tests and tearing tests were carried out. Specimen dimension is shown in Figure 1. Each specimen was then cut into 3 pieces according to the numbers ①, ②, and ③. The membrane material in area 1 was used for visual property measurements, scanning electron microscopy tests, and infrared spectroscopy, and the material in areas 2 and 3 was used for mechanical property tests. Then, we can assume that all tested values are the material properties of one specimen. In a word, 40 specimens were obtained from both directions of every group, and 9 variables (properties) were gathered of each specimen, for statistical analysis.

2.2.1. Spectrocolorimetry Characterization.

In comparison to new materials, aged fabrics experienced obvious color changes as a result of dirt adhesion and ultraviolet light. The surface color analysis was performed using a Datacolor SF600 spectrophotometer (United States). As specified, the illuminant chosen in the experiments was D65/10°, A/10°, and F11/10°. The lightness and colors of fabrics were determined in accordance with the CIE 1976 $L*$, $a*$,$b*$ uniform system. This $L*a*b*$ color model is perceptual and allows the measurement of color differences and evolutions. In this system, the $L*$ indicator represents the lightness; meanwhile, $a*$ and $b*$ refer to the chromaticity. The decline of $L*$ (from 100 to 0) illustrates that the material is gradually darkening. Besides, $a*$ and $b*$ are the chromaticity positions on axes from −300 to +300. To be specific, the indicator −$a*$ to +$a*$ means the color from green to red, and −$b*$ to +$b*$ represents the color from blue to yellow. A small piece (50 mm × 50 mm) of the membrane was cut from area 1 of each specimen for spectrocolorimetry characterization. Mean values were obtained from the analysis of three spots of each small piece.

2.2.2. Contact Angle Measurements.

Contact angle θ_0 is defined as the angle between the solid surface and the line tangent to the liquid drop at the contact line [29]. The contact angle is relevant to adhesion and capillary phenomena, which can help to measure the wettability of a material surface [30]. When the contact angle (θ_0) is an acute angle, the solid surface is partial wetting by the liquid; if θ_0 is a zero angle, the liquid will be completely scattered over the surface of solid, which is called complete wetting; if θ_0 is an obtuse angle, it could be called partial nonwetting; and if θ_0 is a straight angle, it indicates completely nonwetting, and the solid surface could be named a perfectly hydrophobic surface [31]. Recent studies considered that the intrinsic wetting threshold should be 65° rather than 90° [32]. As the wetting qualifying parameter, the contact angle was found directly related to printing processes [33], adhesion, heterogeneous nucleation [34], and so on. Additionally, the contact angle has been used to assess the self-cleaning of membrane materials although the relevant theories still need to be improved.

The contact angle was measured by an OCA50Micro automatic contact angle measuring instrument (Dataphysics Germany), using the sessile drop method. A small piece (50 mm × 50 mm) was also cut from area 1 of each specimen for the contact angle experiment, and 40 specimens were taken in each group of fabrics.

2.2.3. Thickness Measurements.

In addition, the thickness of every specimen was measured in accordance with the test method recommended by the specification FZ/T01003-1991 [35]. A YM141 digital fabric thickness gauge was the testing instrument, with a precision of 0.01 mm. For each specimen, 3 measure points were chosen, and their average was considered the thickness. As we know, thick dust adhered to the surface of aged coated fabrics, so each specimen was rinsed and wiped before its thickness was measured [19].

2.2.4. Surface Morphology Characterization.

In order to observe the surface morphology and analyse the microstructural organization of the coating, SEM was carried out using a SNE-3000M setup. All specimens were sputter-coated with gold prior to further characterization. Specimens were observed on their ageing-exposed surface at 30 kV, to analyse the ageing damage, especially the crack pattern and cavities. The specimens were viewed at different magnifications (200, 1500, and 3000x), and microscope images were captured. The microcracks, voids, and particulate matters on the aged coating surface can be observed explicitly through these microscope images. Likewise, a small piece (50 mm × 50 mm) was cut from area 1 of each specimen for the surface morphology characterization.

2.2.5. Mechanical Property Tests.

After experiments of physical properties and surface morphology characterization, uniaxial tensile tests and tearing tests were carried out to study the mechanical properties, including tensile strength, tearing strength, uniaxial Young's modulus, and strain at break. Three groups of aged PVDF-coated fabrics were selected as the research object, as shown in Table 1. The unaged fabrics were taken as a spare material group for contrast.

TABLE 1: Detailed information about tested PVDF-coated fabrics.

| Group number	Whether used in structure	Structure name	Structure photo	Ageing time	Structure location
0	No			0	
1	Yes	Zhengzhou Hanhai Stadium Stand membrane structure		15 years (2002~2017)	Zhengzhou
2	Yes	Hangzhou Natatorium roof membrane structure		16 years (1999~2015)	Hangzhou
3	Yes	Nanjing International Exhibition Centre tensile membrane structure		19 years (2000~2019)	Nanjing
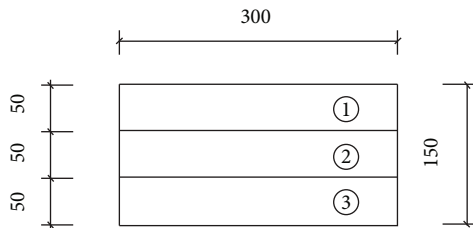
FIGURE 1: Specimen dimension for a series of experiments.

(1) Uniaxial Tensile Tests. The most frequently used method to test mechanical properties of coated fabrics is the uniaxial tensile test. In this research, a SANS-CMT4204 testing machine (Shenzhen, China) was used. Tested fabrics are orthotropy, so each group of fabrics was split into two batches along both directions. Forty specimens were employed in every batch. A detailed illustration of the uniaxial tensile specimen is shown in Figure 2. The length of the rectangular specimen was 300 mm, and the width was 50 mm. Besides, the length of the clamp area was 50 mm. The loading rate of the uniaxial tensile test was 100 mm/min, according to DG/TJ08-2019-2007 [36]. Tensile strength and strain at break were obtained.

Moreover, uniaxial Young's modulus can be calculated through uniaxial cyclic tensile tests. At present, there is no definite experimental method for the elastic modulus of

membrane materials, and different countries adopt different standard suggestions. The uniaxial cyclic tensile test and biaxial tensile test are commonly used. Due to the limited area of aged materials, the uniaxial cyclic tensile test method was adopted in this paper according to MSAJ/M-02 [37]. The experimental steps are described as follows: Firstly, stretch the specimen to σ_{max} (i.e., one-fourth of the smaller failure force in two directions) and unload the force to zero. Secondly, repeat this procedure for five times and fit the last stress-strain tensile curve into a straight line; then, its slope is taken as the value of uniaxial Young's modulus. In each group, repeat the experiment on the forty specimens and calculate uniaxial Young's modulus.

(2) Tearing Tests. Tearing tests were performed by the machine SANS-CMT4204, as well. As shown in Figure 3, the specimen was prepared as a rectangle of 180 mm × 50 mm with an isosceles trapezoid on it. The area out of the trapezoid was marked as shadow because it would be clamped during the test. In the centre of the short base, a small cut of 25 ± 0.5 mm was made in the perpendicular direction. During the test, the trapezoid specimen was clamped along the unparallel edges. Therefore, the short side of the specimen was kept tensioned, and the long side was folded at first. When the clamps on both sides started moving, an increasing load was applied to the specimen, and the specimen was torn along the incision until it was torn totally.
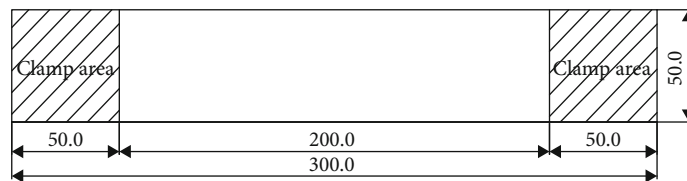
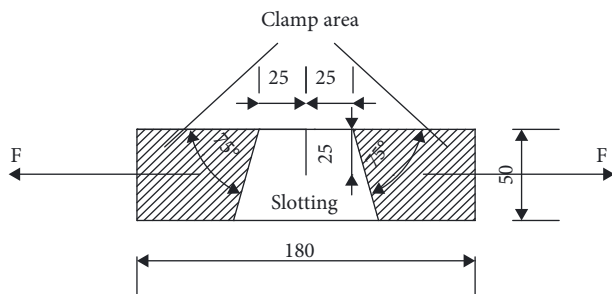Figure 2: Detailed illustration of uniaxial tensile specimen (mm).

Figure 3: Specimen dimension of tearing tests (mm).

The rate of tensile loading was set as 100 mm/min, based on DG/TJ08-2019-2007.

In essence, tearing strength is a statistical result of the fracture force of a single fibre. As demonstrated in Figure 4, the tearing force-displacement curve consists of successive peaks and troughs alternatively. For each recorded tearing curve of the specimen, the mean value of the five maximum load peaks is calculated as the tearing strength. The load peaks are recorded by black and red dots for warp and weft directions, respectively, as shown in Figure 4.

2.2.6. Fourier Transform Infrared Spectroscopy. At present, researches about the micromolecular structure of aged fabrics after engineering applications are relatively scarce. Infrared spectroscopy technique was used to identify the molecular structure and further study the degradation mechanism. Fourier Transform Infrared (FTIR) spectra of aged fabrics were obtained by using the EQUINOX 55 spectrometer between 400 cm^{-1} and 4000 cm^{-1}. The resolution of the spectrometer is 0.4 cm^{-1}, and the attenuated total reflection mode is employed. Every specimen was subjected to a careful drying process before tests started.

2.3. Statistical Analysis. Physical and mechanical properties of membrane materials degrade in the long term of exposure, which is common in architectural applications. The degradation test results are analysed by a statistical technique, namely, Principal Component Analysis (PCA). This data analysis method can help simplify some correlated variables into fewer independent principal components (PCs) through variable linear combinations [38]. In other words, this method helps project variables (properties in this paper) living in a multidimensional space onto a smaller subspace with minimal loss of data information. During this process, orthogonal principal axes are built and a representative loading plot can be obtained. PCA is used to analyse correlations between properties in this study.

The angle between variables, which are projected on the loading plot, can give information about the correlations between properties. Specifically, in the representative loading plot, two variables are not correlated at all if they form an angle of 90°. Besides, if they produce an angle less than 90°, the variables are considered positively correlated. The closer the angle is to 0°, the stronger the correlation is. Oppositely, two variables are negatively correlated if the angle between them is more than 90°. When the angle is 180°, two variables are identified as completely negatively correlated.

It is important to note that test data should be transformed to a unit scale (mean = 0 and variance = 1). To be specific, the value of each variable needs to be standardized by centring, and each centred variable is divided by the standard deviation, as illustrated in equation (1). In this way, the difference of units between all the properties can be eliminated, and the correlations between variables can be analysed:

$$P_i' = \frac{P_i - \bar{P}}{\sigma_P}. \tag{1}$$

In this equation, P_i is the variable and $\bar{P}$ and σ_P are the mean value and standard deviation of the variable P, respectively. P_i' is the centred-reduced variable. The designations of variables (properties) are explained in Table 2.

3. Results and Discussions

A systematic process to evaluate aged membrane materials include visual observations, specimen collection, and laboratory analysis (spectrocolorimetry characterization, contact angle measurements, FTIR spectroscopy, mechanical characterization, and so on). In this section, changes in the macroproperties and microstructures of aged fabrics were discussed and the correlations between properties were studied. As is well known, several prediction models are set up based on elementary processes, such as the Arrhenius law [39] or Schwarzschild law [40]. Besides, results by some researches [41–43] have illustrated that evolutions in chemical structures of engineering materials can reflect their degradation mechanism more effectively. Moreover, macroproperties of materials are pertinent to multilevel structures [44], such as chain structures, aggregation states, macroscopic structures, or surficial cracks. Correlation between physical and mechanical properties are required to study the durability of polymers.
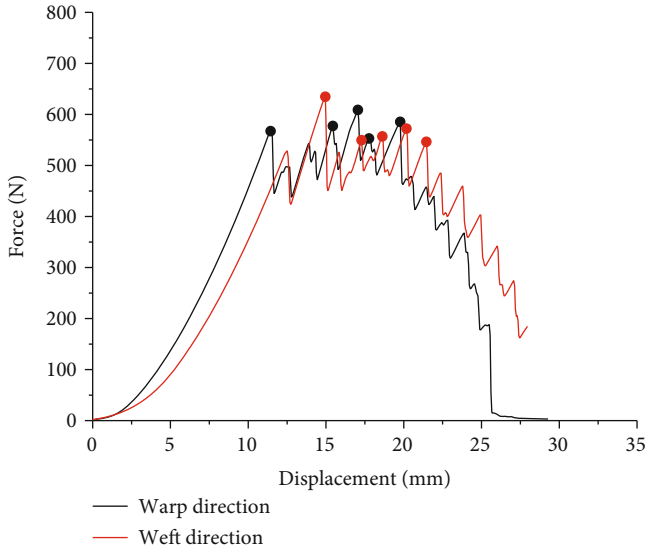
Figure 4: Force-displacement curve of the tearing test.

Table 2: Designation of parameters.

Variable	Parameter
σ	Tensile strength (N/5 cm)
ε	Strain at break (%)
τ	Tearing strength (N)
E	Uniaxial Young's modulus (N/mm)
CA	Contact angle (°)
Th	Thickness (mm)
$L*$	Lightness (light-dark)
$a*$	Chromatic coordinate (red-green)
$b*$	Chromatic coordinate (yellow-blue)

It is worth mentioning that semiquantitative relationships are also helpful when the measurement of mechanical properties is not possible due to the limitation of specimen size [45].

3.1. Physical Performance Degradation

3.1.1. Visual Appearance Change. Weathering had a great impact on the visual appearance of PVDF-coated fabrics. All specimens underwent a similar process of surface evolution, that is, becoming stained, slight yellow, and dark yellow. It is obvious that specimens of group 3 show the most remarkable yellow. The digital photos of fabrics before and after degradation are shown in Figure 5. The membrane materials of group 2 were coated with silver coating, due to the requirements of building appearance modelling. A significant ageing phenomenon can be observed on the surface coating. As we can see, the surface of aged fabrics lost luster and turned yellow and darkened, while the stains and spots can also be observed.

In order to investigate the visual appearance change more scientifically, the surface color analysis was performed. The CIE $L*$, $a*$,$b*$ color system was employed to deter-

mine the lightness and the color. Mean values were calculated from the analysis of three points of each specimen, and every group had 40 specimens. Test results and chromaticity data evolution are illustrated in Table 3.

For each group of coated fabrics, the spectrocolorimetry characterization was performed under D65/10°, A/10°, and F11/10°, respectively. It can be found from Table 3 that there is little difference in the color analysis test results under different optical sources. $DL*$ is the difference between brightness values, which is $DL* = L_n - L_0$. When $DL*$ is negative, it means the color of the aged specimen is darkened. The larger the absolute value is, the more the change is. Besides, Da is the difference between green-red chromaticity, which is $Da = a_n - a_0$. When Da is positive, it indicates the color of the aged specimen gradually turns red. Db is the difference between blue-yellow chromaticity, which is $Db = b_n - b_0$. When Db is positive, it indicates that the color of the aged specimen gradually turns yellow. Total color difference DE is a comprehensive reflection of various color difference values. DE can be calculated according to equation (2). The greater the value of DE is, the greater the total color difference is:

$$DE = \sqrt{DL*^2 + Da^2 + Db^2}. \qquad (2)$$

After degradation for more than ten years in the natural environment, the surface of membrane materials gradually darkens. As ageing time increases, the $L*$ coordinate gradually decreases, meaning the brightness weakens. Besides, the $a*$ and $b*$ coordinates both show a rising trend compared with the unaged material (group 0). It means the color of the aged fabrics gradually turns red and yellow, which is consistent with the phenomena observed by naked eyes. Fabrics of group 3 produce the most remarkable surface change, since DE of group 3 is the largest.

The aged coated fabrics of group 1, group 2, and group 3 were removed from real membrane structures in different cities, which were subjected to different stress states and different climate environments. The degradation of coated fabrics can be considered the accumulation of environmental factors and loads. The ultraviolet radiation and the temperature mainly affect the coating appearance and the mechanical properties of yarns, while the stress can change the crimp degrees of yarns and decrease the coating thickness. Different environment and stress circs of engineering structures can be considered the factors that affect the ageing of materials.

3.1.2. Contact Angle Evolution. The contact angle of the material surface is an important measurable parameter about wettability, which can reflect resistance against ageing of coated fabrics. Coated fabrics used for membrane structures are considered hydrophobic, which means part of dust can automatically fall from the surface, due to rain erosion and wind blowing. When the contact angle is between 0° and 90°, the smaller the angle, the worse the hydrophobicity.

Representative experimental images of contact angles are shown in Figure 6. Mean values and standard deviations of contact angles are illustrated in Table 4. With the ageing

(a) unaged fabrics of Group 0

(b) aged fabrics of Group 1

(c) aged fabrics of Group 2
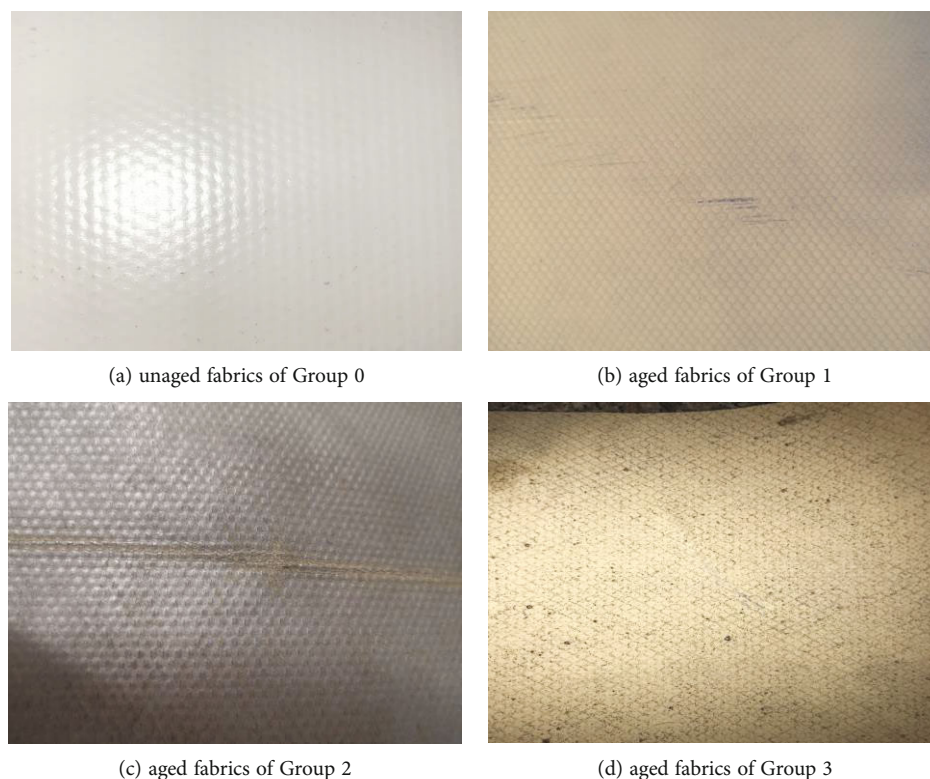

(d) aged fabrics of Group 3

FIGURE 5: Digital photos of PVDF-coated fabrics before and after degradation: (a) unaged fabrics of group 0, (b) aged fabrics of group 1, (c) aged fabrics of group 2, and (d) aged fabrics of group 3.

TABLE 3: Chromaticity data evolution of experimental PVDF-coated fabrics.

Group	Optical source	$L*$	$a*$	$b*$	$DL*$	$Da*$	$Db*$	DE
0	D65/10°	94.94	-1.13	1.73	—	—	—	—
	A/10°	94.94	-0.29	1.31	—	—	—	—
	F11/10°	94.90	-0.62	1.60	—	—	—	—
1	D65/10°	76.19	0.07	2.76	-18.75	1.20	1.03	18.82
	A/10°	76.39	0.72	2.88	-18.55	1.01	1.57	18.64
	F11/10°	76.33	0.23	3.10	-18.57	0.85	1.50	18.65
2	D65/10°	69.71	6.10	20.57	-25.23	7.23	18.84	32.31
	A/10°	71.66	10.04	22.62	-23.28	10.33	21.31	33.21
	F11/10°	70.90	6.37	23.26	-24.00	6.99	21.66	33.08
3	D65/10°	65.31	9.14	23.98	-29.63	10.27	22.25	38.45
	A/10°	66.71	11.63	25.64	-28.23	11.92	24.33	39.13
	F11/10°	65.82	9.87	26.86	-25.08	10.49	25.26	37.11

time increasing, the contact angle of coated fabrics becomes smaller, and the hydrophobic property gets weaker. Thus, the antifouling and self-cleaning property of aged fabrics cannot achieve the expected effect. The service life of membrane materials is shortened, and finally, the material has to

be replaced. Besides, the standard deviation of contact angle rises with ageing time increasing. The increase of standard deviation means the increase of data dispersion and the uncertainty of material apparent properties. Therefore, the contact angle can reflect the ageing degree and service life of coated fabrics to some extent.

3.2. Mechanical Performance Deterioration

3.2.1. Tensile Strength and Tearing Strength. Mean values (MV) and retention rates (RR) of mechanical properties are illustrated in Table 5. Tensile strength and tearing strength are the focal point for durability analysis. From group 0 to group 3, there is a significant decline for each mechanical property index, indicating that ageing time is a main influencing factor for material deterioration. As shown in Table 5, mechanical properties of tested fabrics along warp and weft directions are obviously different. The indicators, including strengths and Young's moduli in both directions, show no obvious variety regulation. Experimental results reveal that the aged materials' uniaxial tensile strengths retain 57.5%-88.2% of the unaged fabrics, while the retention rates of strain at break range from 72.3% to 83.8%. According to Chinese standard CECS158: 2015 [46], the difference of coated fabrics' uniaxial tensile strength between two directions should be no more than 20%. Tensile strengths of unaged PVDF-coated fabrics (group 0) comply with the regulation of CECS158: 2015. Aged PVDF-coated fabrics of groups 1, 2, and 3, however, do not satisfy the
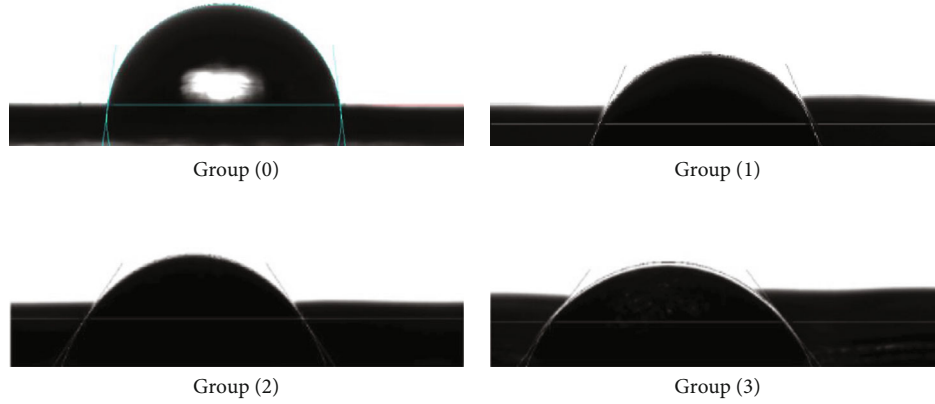
Group (0)

Group (1)

Group (2)

Group (3)

Figure 6: Representative experimental images of contact angles of PVDF-coated fabrics.

Table 4: Contact angle evolution of experimental PVDF-coated fabrics.

Group number	Mean values of contact angles	Standard deviations of contact angles
0	86.10°	2.05°
1	67.36°	4.12°
2	55.64°	5.22°
3	48.19°	7.06°

standard requirement. Furthermore, the tearing strength of coated fabrics should be larger than 7% of the standard value of ultimate tensile strength multiplied by 1 centimeter [46]. All groups of materials including unaged and aged fabrics conform to the standard. It can also be found from Table 5 that the retention rate of the tearing strength is lower compared with the tensile strength in most cases, which is in accordance with other papers [16, 47]. Degradation of tearing strength is more evident than that of tensile strength, especially in the warp direction. Hence, in order to prolong the coated fabrics' service life, it is essential to improve the tearing strength and reduce cracks.

In addition, Young's moduli of aged coated fabrics are smaller than those of unaged fabrics without exception. The aged specimens' uniaxial Young's moduli keep 71.3%-88.7% of unaged fabrics. But requirements for unaged coated fabrics' mechanical properties and the retention rates of aged fabrics are not stated in the present Chinese specifications. More test data about aged fabrics need to be cumulated to make up for the specification's deficiency.

3.2.2. Tensile Property Statistical Analysis. Box plots of tensile strengths and the standard deviation of each group of test data are illustrated in Figure 7. The average tensile strength of unaged specimens in the warp direction was 5586.4 N/5 cm. After being used in engineering structures for 15, 16, and 19 years, the fabrics' tensile strength suffered a reduction of 11.8%, 22.9%, and 24.2% to 4925.5 N/5 cm, 4304.4 N/5 cm, and 4238.0 N/5 cm, respectively. Similarly, the tensile strength in the weft direction dropped from 5027.0 N/5 cm to 3911.5 N/5 cm, 2894.0 N/5 cm, and

2890.7 N/5 cm. These test results reveal that ageing time is the main factor leading to the decrease of tensile strength. It can be inferred that there exists a relationship between degraded tensile strength and ageing time, which has not been confirmed at present. According to a research about the artificial accelerated ageing test [47], during the initial weathering period, the degradation rate of tensile strength is relatively fast. With the prolongation of ageing time, material degradation gradually decelerates.

Moreover, Figure 7 demonstrates phenomenal growth in the standard deviation of tensile strength. The mechanical properties of membrane materials are influenced by the manufacturing process, and their diversity is generally larger than that of metals. The uncertainty of mechanical properties of coated fabrics is due to many factors such as impurities, voids, incomplete curing, and imperfect bonding. Standard deviation increases significantly over the ageing time, meaning the discrete degree of test data gets higher. Thus, it is not scientific to use the average values of tensile strength as the evaluation index. Therefore, reliability calculation should be introduced in the durability design of membrane structures.

3.2.3. Tearing Property Statistical Analysis. For tensile membrane structures, sudden destruction caused by tear and crack propagation is catastrophic, which is one of the most common failure modes. Therefore, the tearing resistance of coated fabrics is an important research object. Considering the uncertainty of material properties, damages from construction, and environmental influence, a relatively large safety margin is required for coated fabrics. In membrane structural design, large safety factors are applied, usually 5~7 for the tensile strength [48]. However, PVDF-coated fabrics in common use usually have high tensile strength and comparatively low tearing strength.

Box plots of tearing strength and standard deviation of each group of test data are illustrated in Figure 8. Experimental results show that mean values of tearing strength decreased apparently while the standard deviation had remarkable growth. The average tearing strength of unaged specimens in the warp direction was 847 N. After ageing for 15, 16, and 19 years, the fabrics' tearing strength retained

TABLE 5: Mechanical properties (mean value and retention rate) of experimental coated fabrics.

| Group number		Tensile strength (N/5 cm)		Strain at break (%)		Tearing strength (N)		Uniaxial Young's modulus (N/mm)	
		Warp	Weft	Warp	Weft	Warp	Weft	Warp	Weft
0	MV	5586.4	5027.0	23.4	21.7	847	691	513.2	493.8
1	MV	4925.5	3911.5	19.6	18.1	648.3	529.8	455.2	410.2
	RR	88.2%	77.8%	83.8%	83.4%	76.5%	76.7%	88.7%	83.1%
2	MV	4304.4	2894.0	18.4	17.2	627.6	503.2	393.9	365.2
	RR	77.1%	57.6%	78.6%	79.3%	74.1%	72.8%	76.7%	73.9%
3	MV	4238.0	2890.7	17.3	15.7	604.8	498.5	380.9	352.1
	RR	75.8%	57.5%	73.9%	72.3%	71.4%	72.1%	74.2%	71.3%

(a)

(b)
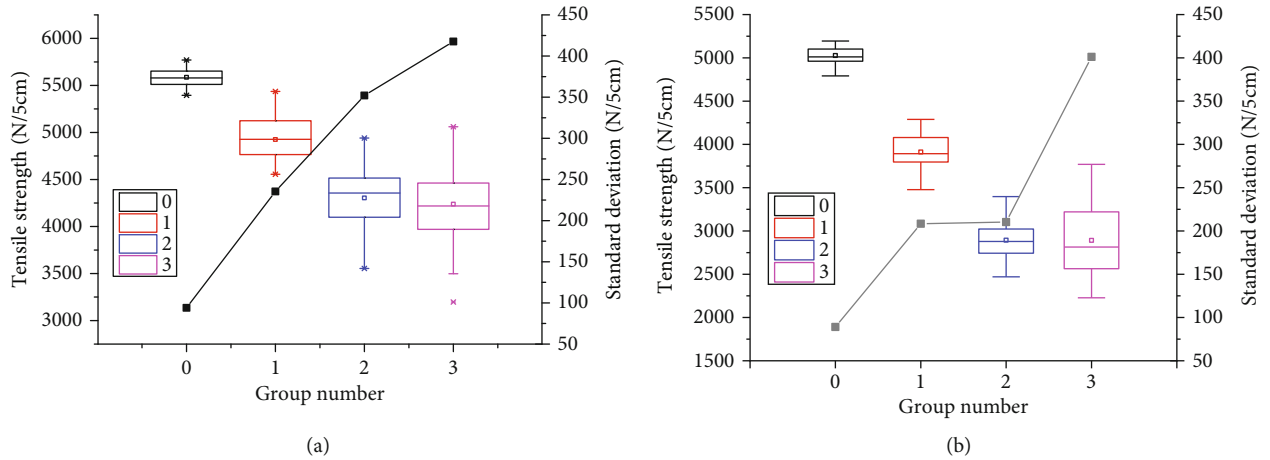
FIGURE 7: Box plots of tensile strength and the standard deviation of each group of test data: (a) test data in warp direction and (b) test data in weft direction.
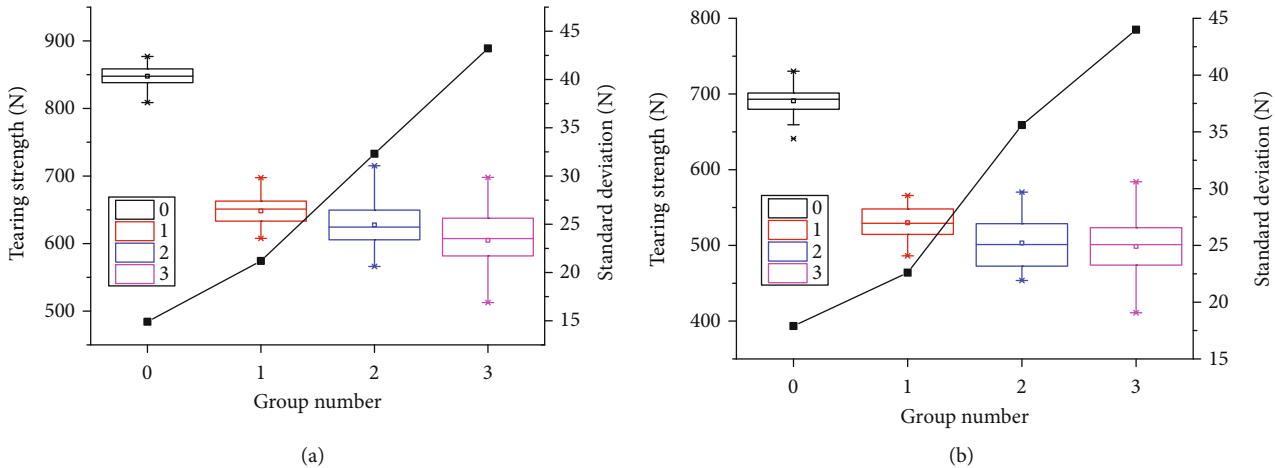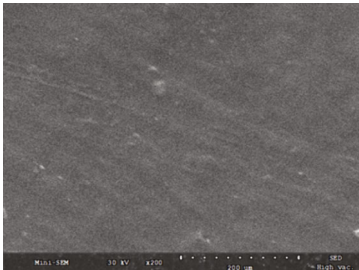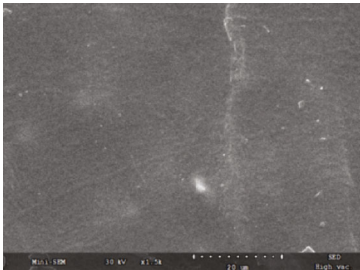

(a)

(b)
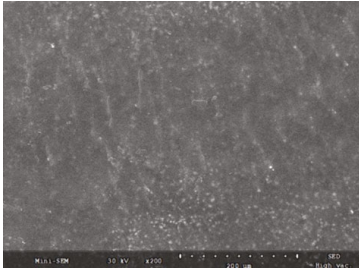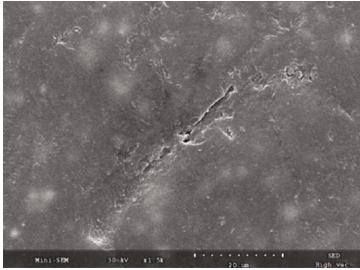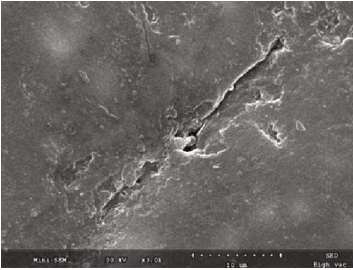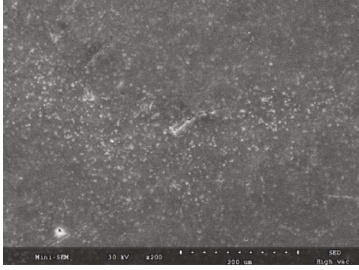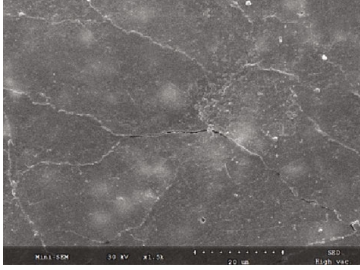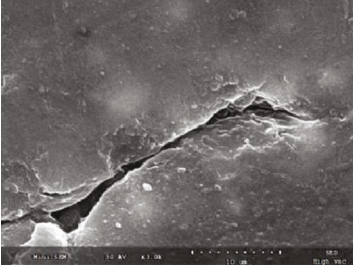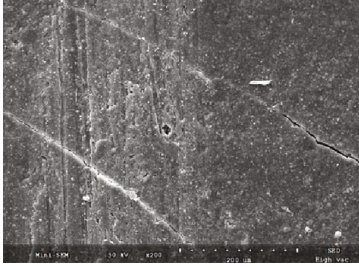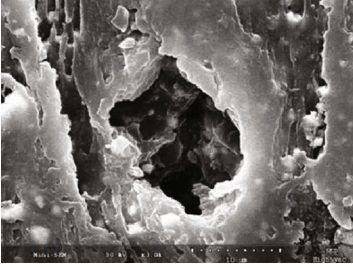
FIGURE 8: Box plots of tearing strength and the standard deviation of each group of test data: (a) test data in warp direction and (b) test data in weft direction.
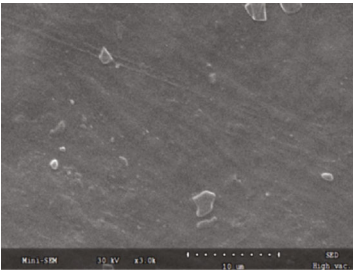
76.5%, 74.1%, and 72.1% of the unaged fabrics and dropped to 648.3 N, 627.6 N, and 604.8 N, respectively. Similarly, the tearing strength of specimens in the weft direction fell from 691 N to 529.8 N, 503.2 N, and 498.5 N. The substantial rise of standard deviation means the diversity of tearing strength gets larger during service time. Thus, aged fabrics could be ruptured more easily under tearing stress,

and crack propagation is more likely to be induced even under small loads.

3.3. Surface Morphology. As for polymers, degradation of mechanical properties is usually accompanied by evolutions of physical and chemical properties. Chalking, blistering, peeling, and cracking are all possible surface damages related to

TABLE 6: Scanning micrographs of coated fabric surface performed at 200, 1500, and 3000x.

Group number	Surface micrographs 200x (a)	Surface micrographs 1500x (b)	Surface micrographs 3000x (c)
0			
1			
2			
3			

ageing of coated fabrics. In order to evaluate the surface morphology, especially the crack pattern and cavities, SEM images were taken at different magnifications (200, 1500, and 3000x). Scanning micrographs of coated fabrics are shown in Table 6.

Comparing surface micrographs performed at 200x from 0(a) to 3(a), the specimen of group 0 shows a smooth surface whereas other aged specimens present chalking, blistering, and cracking to varying degrees. The number, width, and depth of microcracks increase significantly with the ageing time extending. Cracking and peeling of the coating are most obvious on the specimens of group 3. Surface micrographs 0(b) and 0(c) reveal that adherence of airborne particulates exists even for unaged coated fabrics.

Moreover, crack density and crack size of group 1 turn out to be smaller, among aged specimens. Making a comparison from profile 0(b) to 3(b), it can be inferred that transverse cracks were initiated at first, and the cracks got larger and dee-

per as ageing time prolonged; meanwhile, new fine cracks emerged between them. Besides, several secondary cracks appeared as well and developed from the lateral side of the main cracks. Then, the crack networks constituted, as shown in profile 2(b). The crack growth pattern of three groups of aged fabrics was similar, which means that the crack evolution mechanism is independent of exposure conditions.

As can be seen from image 3(a), there are distinct cracks and voids. In 1500x and 3000x magnification images, one crack and the largest void can be clearly observed. The occurrence of cracks on specimens of group 3 was quite widespread, through which rain, oxygen, and ultraviolet radiation can access the interior fibres more easily. Degradation of physical and mechanical properties of specimens in group 3 is most serious, compared to other specimens in group 1 and group 2. These results are in accordance with the change of contact angle (CA parameter), tensile strength,
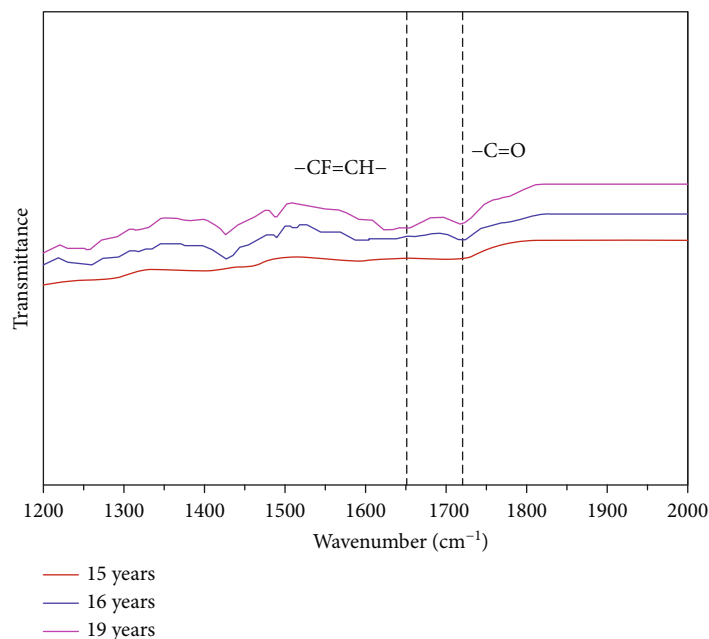
FIGURE 9: FTIR spectra in the region of 1200-2000 cm^{-1} for the exposed surface of specimens during service time (15 years, 16 years, and 19 years).
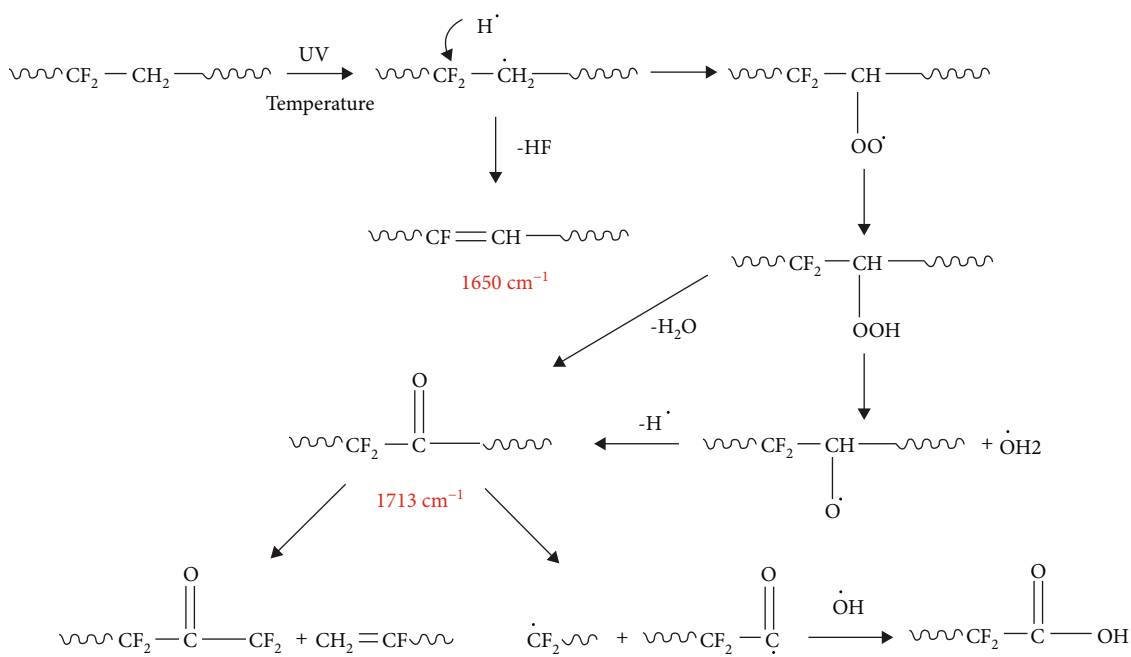
FIGURE 10: Degradation mechanism of PVDF during service time.

and tearing strength. Therefore, surface morphology can reflect the degradation of physical and mechanical properties of coated fabrics.

3.4. Molecular Structure Characterization. In order to characterize the molecular structure of aged fabrics, infrared spectra were systematically measured. FTIR spectra in the region between 1200 cm^{-1} and 2000 cm^{-1} for the aged specimens are

mainly focused on. As shown in Figure 9, one characteristic absorption peak has appeared at 1650 cm^{-1}, which is caused by the -CF=CH- stretching vibration. Meanwhile, another characteristic absorption peak also appeared at 1720 cm^{-1}, resulting from the carbonyl stretching vibration produced by the oxidation reaction. There have been some studies on the degradation process of PVDF, which mainly includes oxidation reaction and the decomposition of HF [49–52].

(a) Group 0

(b) Group 1

(c) Group 2

(d) Group 3

FIGURE 11: Representative loading plot of PCA correlation between properties: (a) group 0, (b) group 1, (c) group 2, and (d) group 3.

TABLE 7: Coefficient matrix of unaged PVDF-coated fabrics (group 0).

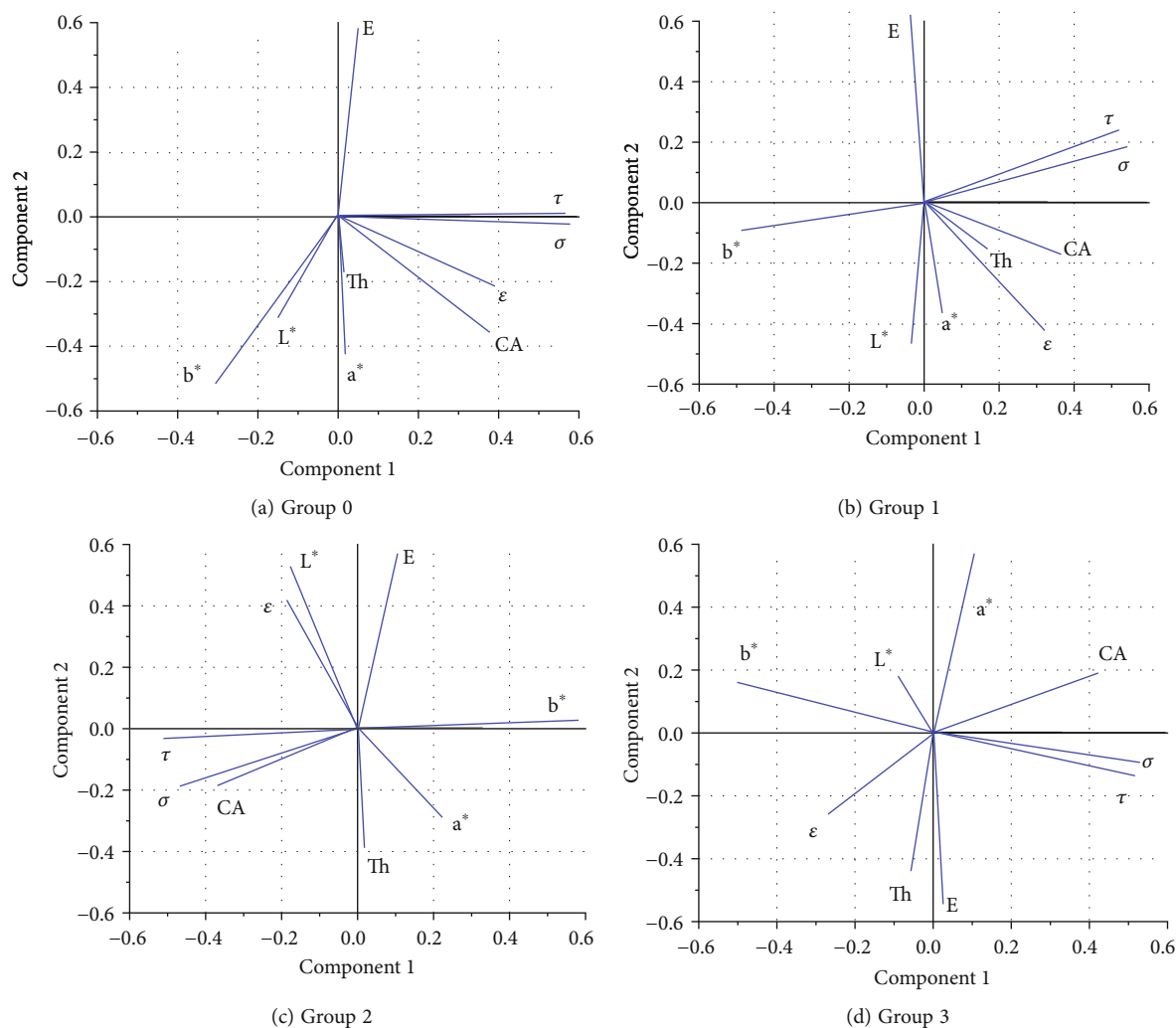| Variable	σ	ε	τ	E	CA	Th	$L*$	$a*$	$b*$
σ	1	0.421	0.912	0.126	0.796	-0.035	0.385	-0.303	-0.748
ε	0.421	1	0.336	0.117	0.316	-0.089	0.124	-0.044	-0.492
τ	0.912	0.336	1	0.129	0.767	-0.098	0.159	-0.272	-0.769
E	0.126	0.117	0.129	1	0.019	-0.133	-0.252	-0.097	0.004
CA	0.796	0.316	0.767	0.019	1	-0.163	0.104	0.268	-0.7
Th	-0.035	-0.089	-0.098	-0.133	-0.163	1	0.456	-0.144	0.079
$L*$	0.385	0.124	0.159	-0.252	0.104	0.456	1	0.192	-0.052
$a*$	-0.303	-0.044	-0.272	-0.097	0.268	-0.144	0.192	1	0.022
$b*$	-0.748	-0.492	-0.769	0.004	-0.7	0.079	-0.052	0.022	1

In the molecular structure of PVDF, C-F and C-H bonds are distributed on the main chain, and their bond energies are 485.9 kJ/mol and 413.0 kJ/mol, respectively. Therefore, the degradation mechanism of PVDF during service time can be described as follows. As shown in Figure 10, under the action of solar ultraviolet radiation (the energy range of

ultraviolet at 200-400 nm is 598-301 kJ/mol), the CH_2 of PVDF is easy to dehydrogenize and becomes free radical, which combines with F on the neighbouring C atom and dissociates HF to form -CF=CH-. The action of these chromophores causes the color of fabrics to turn yellow gradually. At the same time, the free radical can also combine with

TABLE 8: Coefficient matrix of aged PVDF-coated fabrics (group 1).

Variable	σ	ε	τ	E	CA	Th	$L*$	$a*$	$b*$
σ	1	0.376	0.828	0.172	0.718	-0.09	0.147	-0.213	-0.754
ε	0.376	1	0.276	0.1	0.268	0.293	0.035	-0.087	-0.529
τ	0.828	0.276	1	0.074	0.616	-0.232	0.165	-0.239	-0.625
E	0.172	0.1	0.074	1	0.295	0.135	0.142	0.263	0.011
CA	0.718	0.268	0.616	0.295	1	-0.083	-0.049	-0.118	-0.479
Th	-0.09	0.293	-0.232	0.135	-0.083	1	-0.106	0.071	0.071
$L*$	0.147	0.035	0.165	0.142	-0.049	-0.106	1	0.059	-0.192
$a*$	-0.213	-0.087	-0.239	0.263	-0.118	0.071	0.059	1	0.139
$b*$	-0.754	-0.529	-0.625	0.011	-0.479	0.071	-0.192	0.139	1

TABLE 9: Coefficient matrix of aged PVDF-coated fabrics (group 2).

Variable	σ	ε	τ	E	CA	Th	$L*$	$a*$	$b*$
σ	1	0.315	0.877	0.102	0.788	-0.218	0.063	-0.216	-0.797
ε	0.315	1	0.407	-0.227	0.26	0.094	0.357	-0.185	-0.011
τ	0.877	0.407	1	0.096	0.795	-0.155	0.017	-0.149	-0.719
E	0.102	-0.227	0.096	1	0.09	0.068	-0.048	0.175	-0.159
CA	0.788	0.26	0.795	0.09	1	0.208	-0.059	0.26	-0.878
Th	-0.218	0.094	-0.155	0.068	0.208	1	-0.043	0.2	-0.175
$L*$	0.063	0.357	0.017	-0.048	-0.059	-0.043	1	-0.121	0.092
$a*$	-0.216	-0.185	-0.149	0.175	0.26	0.2	-0.121	1	-0.304
$b*$	-0.797	-0.011	-0.719	-0.159	-0.878	-0.175	0.092	-0.304	1

oxygen to form a peroxyl radical, which forms a carbonyl after rearrangement and dehydration. As a consequence, the stretching vibration peak at $1720\,\text{cm}^{-1}$ gradually enhanced and the degree of oxidation deepened. Under the combined action of temperature and ultraviolet, the oxidized PVDF could continue to react and fracture. Therefore, the mechanical properties of PVDF-coated fabrics gradually decrease during the service time of membrane structures.

3.5. Multivariate Correlation Analysis. In this section, all the properties of PVDF-coated fabrics are analysed through the PCA method, in order to establish correlations between mechanical and physical properties. The correlations between properties of 4 groups of experimental fabrics are depicted in Figure 11. This plot helps make clear the relationships among properties by estimating the angle formed between their vectors. The centred-reduced experimental data are adopted for the statistical analysis, which has been illustrated in Section 2.3. In this graph, every variable is represented by a vector (nine variables in total). Direction and length of the vector give information about each variable's contribution to the principal components.

In engineering applications, tensile strength and tearing strength are always the focal point for structural design. As can be seen from Figures 11(a)–11(d), a small angle between tensile strength (σ) and tearing strength (τ) vectors is raised

without exception, so they are extremely correlated. Indeed, both the tensile strength and tearing strength decrease significantly with the weathering. Besides, for all the aged coated fabrics, an anticorrelation between mechanical properties (σ, τ) and $b*$ (yellow-blue chromatic coordinate) is observed. Therefore, the mechanical property loss (tensile strength and tearing strength decrease) could be quantitatively linked to the $b*$ increase since they are opposed.

Moreover, we can see that CA (contact angle) displays a close correlation with the two components of mechanical properties (σ, τ). As mentioned above, the contact angle became smaller evidently with the increase of service time. The positive correlation raised between CA and σ, τ suggests that the mechanical properties are linked to the surface state of specimens. It can be inferred that microcracks and hollows appearing on the surface during ageing may lead to the decrease of tensile strength and tearing strength.

It is quite evident from Figure 11(a) that strain at break (ε) and tearing strength form an angle less than 45°, meaning they are positively correlated for unaged fabrics. This is consistent with the research of Hager et al. [53], which proposed a general equation relating the tearing strength to the elongation at break of a given fabric. However, we can see from Figures 11(b)–11(d) that the angle between strain at break (ε) and tearing strength enlarges with ageing time increasing. For aged fabrics, strain at break (ε) and tearing strength

TABLE 10: Coefficient matrix of aged PVDF-coated fabrics (group 3).

Variable	σ	ε	τ	E	CA	Th	$L*$	$a*$	$b*$
σ	1	0.394	0.885	0.071	0.855	-0.006	0.236	-0.24	-0.827
ε	0.394	1	0.37	0.157	0.313	0.068	0.078	0.077	-0.298
τ	0.885	0.37	1	0.094	0.827	-0.194	0.166	-0.261	-0.783
E	0.071	0.157	0.094	1	0.106	0.1	-0.242	0.082	0.055
CA	0.855	0.313	0.827	0.106	1	-0.231	0.19	0.193	-0.913
Th	-0.006	0.068	-0.194	0.1	-0.231	1	-0.083	-0.021	0.232
$L*$	0.236	0.078	0.166	-0.242	0.19	-0.083	1	0.056	-0.294
$a*$	-0.24	0.077	-0.261	0.082	0.193	-0.021	0.056	1	-0.128
$b*$	-0.827	-0.298	-0.783	0.055	-0.913	0.232	-0.294	-0.128	1

cannot be considered positively correlated, since the extensibility of the fibres is affected during the ageing process.

Coefficient matrixes of unaged PVDF-coated fabrics (group 0) and aged fabrics (groups 1-3) were obtained through PCA and shown in Tables 7–10. Mechanical properties of membrane materials are important factors to ensure the accuracy of the design, analysis, and evaluation of membrane structures. As can be seen from Tables 7–10, the correlation coefficient between σ and τ is the largest (>0.8), indicating that there is a significant correlation between tensile strength and tearing strength. Besides, contact angle (CA) and yellow-blue chromatic coordinate $b*$ are the performance indexes whose correlation coefficient (absolute value) with σ is greater than 0.5. The results demonstate that contact angle (CA) has a positive correlation with tensile strength, while the yellow-blue chromatic coordinate $b*$ has a negative correlation with tensile strength. Similarly, contact angle (CA) and yellow-blue chromatic coordinate $b*$ are also the indexes whose correlation coefficient (absolute value) with τ is greater than 0.5. It indicates that contact angle (CA) was positively correlated with the tearing strength, while the yellow-blue chromatic coordinate $b*$ was negatively correlated with the tearing strength. These conclusions are consistent with the results of the correlation analysis above.

During the service period of membrane structures, it is unreasonable to perform destructive tests of membrane materials. These results provide additional methods to evaluate in-place membrane materials of an engineering structure. Considering that tensile tests and tearing tests are destructive, $b*$ and CA can be used as the index to predict mechanical properties of membrane materials and to evaluate the ageing degree of membrane materials. It provides a reference method for evaluating in situ membrane materials of existing membrane structures. It is well known that molecular structure changes and chain scissions of polymers can lead to degradation of their appearance and physical and mechanical properties. Lv et al. [54] studied the relationship between molecular weight and tensile strength of isotactic polypropylene (iPP), which was found to be consistent with an empirical linear model. However, the experimental research on molecular weight of PVDF-coated fabrics has

not been done in this paper, which is the next research direction.

4. Conclusions

In order to guarantee the service life of membrane structures, the degradation during the lifetime of membrane materials is a question which deserved consideration. This paper studies the ageing behaviour of PVDF-coated fabrics after practical engineering applications, by investigating the microstructure, physical properties, and mechanical properties based on statistical analysis. Three groups of aged coated fabrics, taken from different engineering structures in China, are tested and analysed.

Spectrocolorimetric measurements report that $L*$ increase and $b*$ decrease after weathering. It means that the membrane surface darkens and turns yellow. Contact angle and thickness measurements are also used to characterize the physical properties. The surface of aged fabrics gets cracked and sticky, resulting in the cleaning difficulty of the materials. Furthermore, the images taken by SEM permit us to observe the degradation of the materials. Then, comprehensive test data of mechanical properties are collected. The aged fabrics lost some of their initial mechanical properties, especially the tensile strength and tearing strength. These properties are considered essential in the estimation of the long-term behaviour of coated fabrics. In addition, retention rates of mechanical properties compared with unaged coated fabrics are also calculated and listed. Degradation of aged fabrics' tearing strength is found to be more obvious than tensile strength. Fourier Transform Infrared spectrum analysis was employed to characterize the molecular structure of PVDF.

Moreover, the mechanical properties of aged PVDF-coated fabrics still conform to normal distribution. Although the curve representing the relationship between tensile strength and ageing time cannot be confirmed, the overall variation trend can be known. During the service life of membrane materials, mean values of tensile strength decrease while standard deviations increase, meaning the uncertainty of material properties augments. Thus, the reliability of material performance degenerates significantly,

and the load-carrying capacity of coated fabrics is affected unfavourably. These data uncertainties of mechanical properties should be taken into account for reliability calculation in the durability design of membrane structures.

Another objective of this paper is to provide analysis methods to evaluate in-place membrane materials. The PCA showed an anticorrelation between mechanical properties (σ, τ) and $b*$ (yellow-blue chromatic coordinate) for all the 3 groups of aged fabrics. Also, the positive relation between CA (contact angle) and the mechanical properties (σ, τ) suggests that mechanical properties are related to the surface state. Considering that experiments on mechanical properties (tensile tests, tearing tests) are destructive to membrane materials, $b*$ and CA can be used as the predictive indicator of coated fabrics during the service life. This type of indicator may provide sufficient information to allow for a planned, timely replacement of membrane materials. The study offers a further understanding of aged PVDF-coated fabrics' physicomechanical properties and provides references for the durability evaluation.

Data Availability

The raw/processed data required to reproduce these findings cannot be shared at this time as the data also forms part of an ongoing study.

Conflicts of Interest

The authors declare that they have no conflicts of interest.

Acknowledgments

References

[1] L. Soccalingame, D. Perrin, J.-C. Bénézet, and A. Bergeret, "Reprocessing of UV-weathered wood flour reinforced polypropylene composites: study of a natural outdoor exposure," *Polymer Degradation and Stability*, vol. 133, pp. 389–398, 2016.

[2] A. Ambroziak, "Mechanical properties of Precontraint 1202S coated fabric under biaxial tensile test with different load ratios," *Construction and Building Materials*, vol. 80, pp. 210–224, 2015.

[3] A. Ambroziak and P. Kłosowski, "Mechanical properties for preliminary design of structures made from PVC coated fabric," *Construction and Building Materials*, vol. 50, pp. 74–81, 2014.

[4] M. Wu, Y. Li, and Y. Shang, "Statistical characteristics of ethylene tetrafluoroethylene foil's mechanical properties and its partial safety factors," *Journal of Materials in Civil Engineering- ASCE*, vol. 28, no. 5, article 04016004, 2016.

[5] M. Wu, Y. Shang, and Y. Li, "Biaxial tensile mechanical properties of ETFE foil," *Journal of Building Materials*, vol. 17, no. 4, pp. 623–626, 2014.

[6] W. Tan and B. G. Falzon, "Modelling the crush behaviour of thermoplastic composites," *Composites Science and Technology*, vol. 134, pp. 57–71, 2016.

[7] W. Tan and B. G. Falzon, "Modelling the nonlinear behaviour and fracture process of AS4/PEKK thermoplastic composite under shear loading," *Composites Science and Technology*, vol. 126, pp. 60–77, 2016.

[8] W. Tan, F. Naya, L. Yang et al., "The role of interfacial properties on the intralaminar and interlaminar damage behaviour of unidirectional composite laminates: experimental characterization and multiscale modelling," *Composites Part B: Engineering*, vol. 138, no. December 2017, pp. 206–221, 2018.

[9] V. K. T. Prateek and R. K. Gupta, "Recent progress on ferroelectric polymer-based nanocomposites for high energy density capacitors: synthesis, dielectric properties, and future aspects," *Chemical Reviews*, vol. 116, no. 7, pp. 4260–4317, 2016.

[10] T. Rydzkowski, K. Reszka, M. Szczypiński, M. M. Szczypiński, E. Kopczyńska, and V. K. Thakur, "Manufacturing and evaluation of mechanical, morphological, and thermal properties of reduced graphene oxide-reinforced expanded polystyrene (EPS) nanocomposites," *Advances in Polymer Technology*, vol. 2020, Article ID 3053471, 9 pages, 2020.

[11] A. C. Albuquerque, K. Joseph, L. H. Carvalho, and J. R. M. D'Almeida, "Effect of wettability and ageing conditions on the physical and mechanical properties of uniaxially oriented jute-roving-reinforced polyester composites," *Composites Science and Technology*, vol. 60, no. 6, pp. 833–844, 2000.

[12] N. Guermazi, A. B. Tarjem, I. Ksouri, and H. F. Ayedi, "On the durability of FRP composites for aircraft structures in hygrothermal conditioning," *Composites: Part B*, vol. 85, pp. 294–304, 2016.

[13] A. P. Cysne Barbosa, A. P. P. Fulco, E. S. S. Guerra et al., "Accelerated aging effects on carbon fiber/epoxy composites," *Composites. Part B, Engineering*, vol. 110, pp. 298–306, 2017.

[14] V. K. Thakur, M. K. Thakur, P. Raghavan, and M. R. Kessler, "Progress in green polymer composites from lignin for multifunctional applications: a review," *ACS Sustainable Chemistry & Engineering*, vol. 2, no. 5, pp. 1072–1092, 2014.

[15] K. Zerdzicki, P. Klosowski, and K. Woznica, "Influence of service ageing on polyester-reinforced polyvinyl chloride-coated fabrics reported through mathematical material models," *Textile Research Journal*, vol. 89, no. 8, pp. 1472–1487, 2019.

[16] L. P. Real and J. L. Gardette, "Ageing and characterisation of PVC-based compounds utilised for exterior applications in the building construction field: 1: Thermal ageing," *Polymer Testing*, vol. 20, no. 7, pp. 779–787, 2001.

[17] L. P. Real and J.-L. Gardette, "Ageing and characterisation of PVC-based compounds utilised for exterior applications in the building construction field: 2: artificial accelerated ageing with xenon light," *Polymer Testing*, vol. 20, no. 7, pp. 789–794, 2001.

[18] Y. Li, T. Liu, B. Yang, Q. Zhang, and Y. Zhang, "Effects of natural ageing on mechanical properties of PVDF-coated fabrics," *Structural Engineering International*, vol. 26, no. 4, pp. 348–356, 2016.

[19] B. Yang, Y. Shang, M. Wu, Z. Yu, and X. Qu, "Statistical characteristics of naturally aged PVDF-coated fabrics' mechanical properties and structural reliability index," *Polymer Testing*, vol. 80, p. 106143, 2019.

[20] I. Jakubowicz, "Effects of artificial and natural ageing on impact-modified poly (vinyl chloride) (PVC)," *Polymer Testing*, vol. 20, pp. 545–551, 2001.

[21] J. M. Sousa, J. R. Correia, J. Gonilha, S. Cabral-Fonseca, J. P. Firmo, and T. Keller, "Durability of adhesively bonded joints between pultruded GFRP adherends under hygrothermal and natural ageing," *Composites. Part B, Engineering*, vol. 158, pp. 475–488, 2019.

[22] D. Feng, D. F. Caulfield, and A. R. Sanadi, "Effect of compatibilizer on the structure-property relationships of kenaf-fiber/polypropylene composites," *Polymer Composites*, vol. 22, no. 4, pp. 506–517, 2001.

[23] S. N. Leung, "Thermally conductive polymer composites and nanocomposites: processing- structure-property relationships," *Composites. Part B, Engineering*, vol. 150, pp. 78–92, 2018.

[24] S. D. Tohidi, A. M. Rocha, N. V. Dencheva, and Z. Denchev, "Microstructural-mechanical properties relationship in single polymer laminate composites based on polyamide 6," *Composites. Part B, Engineering*, vol. 153, pp. 315–324, 2018.

[25] J. W. Martin, J. W. Chin, and T. Nguyen, "Reciprocity law experiments in polymeric photo- degradation: a critical review," *Progress in Organic Coatings*, vol. 47, pp. 292–311, 2013.

[26] J. Chin, T. Nguyen, E. Byrd, and J. Martin, "Validation of the reciprocity law for coating photodegradation," *Journal of Coating Technology and Research*, vol. 2, no. 7, pp. 499–508, 2005.

[27] J. S. Fabiyi, A. G. McDonald, M. P. Wolcott, and P. R. Griffiths, "Wood plastic composites weathering: visual appearance and chemical changes," *Polymer Degradation and Stability*, vol. 93, no. 8, pp. 1405–1414, 2008.

[28] Y. Zhang, Q. Zhang, and H. Lv, "Mechanical properties of polyvinylchloride-coated fabrics processed with Precontraint technology," *Journal of Reinforced Plastics and Composites*, vol. 31, no. 23, pp. 1670–1684, 2012.

[29] A. Marmur, "Interfaces at equilibrium: a guide to fundamentals," *Advances in Colloid and Interface Science*, vol. 244, pp. 164–173, 2017.

[30] J. W. Drelich, "Guidelines to measurements of reproducible contact angles using a sessile-drop technique," *Surface Innovations*, vol. 1, no. 4, pp. 248–254, 2013.

[31] J. W. Drelich, L. Boinovich, E. Chibowski et al., "Editorial," *Surface Innovations*, vol. 7, no. 1, pp. 1–3, 2019.

[32] Y. Tian and L. Jiang, "Intrinsically robust hydrophobicity," *Nature Materials*, vol. 12, no. 4, pp. 291-292, 2013.

[33] K. Liu, M. Cao, A. Fujishima, and L. Jiang, "Bio-inspired titanium dioxide materials with special wettability and their applications," *Chemical Reviews*, vol. 114, no. 19, pp. 10044–10094, 2014.

[34] C. Tang, Z. Liu, C. Peng et al., "New insights into the interaction between heavy metals and struvite: struvite as platform for heterogeneous nucleation of heavy metal hydroxide," *Chemical Engineering Journal*, vol. 365, pp. 60–69, 2019.

[35] FZ/T01003-1991, *Test method for thickness of coated fabrics*, Industrial standard of the People's Republic of China, Textile Industry Standardization Institute, China, 1991.

[36] DG/TJ08-2019-2007, *Technical specification for inspection of membrane structures*, Shanghai Construction and Traffic Committee, Shanghai, 2007.

[37] Membrane Structures Association of Japan, "MSAJ/M-02, Testing Method for Elastic Constants of Membrane Materials," in Membrane Structures Association of Japan, Japan, 1995.

[38] M. Ringnér, "What is principal component analysis?," *Nature Biotechnology*, vol. 26, no. 3, pp. 303-304, 2008.

[39] M. Celina, K. Gillen, and R. Assink, "Accelerated aging and lifetime prediction: Review of non-Arrhenius behaviour due to two competing processes," *Polymer Degradation and Stability*, vol. 90, no. 3, pp. 395–404, 2005.

[40] J. W. Martin, J. W. Chin, and T. Nguyen, "Reciprocity law experiments in polymeric photodegradation: a critical review," *Progress in Organic Coating*, vol. 47, no. 3-4, pp. 292–311, 2003.

[41] M. Diepens and P. Gijsman, "Outdoor and accelerated weathering studies of bisphenol A polycarbonate," *Polymer Degradation and Stability*, vol. 96, no. 4, pp. 649–652, 2011.

[42] G. Gutiérrez, F. Fayolle, G. Régnier, and J. Medina, "Thermal oxidation of clay-nanoreinforced polypropylene," *Polymer Degradation and Stability*, vol. 95, no. 9, pp. 1708–1715, 2010.

[43] Y. Lv, Y. Huang, J. Yang et al., "Outdoor and accelerated laboratory weathering of polypropylene: a comparison and correlation study," *Polymer Degradation and Stability*, vol. 112, pp. 145–159, 2015.

[44] C.-S. Li, M.-S. Zhan, X.-C. Huang, and H. Zhou, "Degradation behavior of ultra-high molecular weight polyethylene fibers under artificial accelerated weathering," *Polymer Testing*, vol. 31, no. 7, pp. 938–943, 2012.

[45] M. C. Celina, "Review of polymer oxidation and its relationship with materials performance and lifetime prediction," *Polymer Degradation and Stability*, vol. 98, no. 12, pp. 2419–2429, 2013.

[46] CECS158, *Technical specification for membrane structures*, China Planning Press, China, 2015.

[47] Z. R. Chen, Q. L. Zhang, and W. L. Xue, "Experimental research on mechanical properties of PVC membrane after ageing," in *Proceedings of the International Association for Shell and Spatial Structures*, Wroclaw, Poland, 2013.

[48] B. Forster and M. Mollaert, *European Design Guide for Tensile Surface Structure*, TensiNet, 2004.

[49] L. A. Pesin, V. M. Morilova, D. A. Zherebtsov, and S. E. Evsyukov, "Kinetics of PVDF film degradation under electron bombardment," *Polymer Degradation and Stability*, vol. 98, no. 2, pp. 666–670, 2013.

[50] A. L. Sidelnikova, V. P. Andreichuk, L. A. Pesin et al., "Kinetics of radiation-induced degradation of CF2- and CF-groups in poly (vinylidene fluoride): model refinement," *Polymer Degradation and Stability*, vol. 110, pp. 308–311, 2014.

[51] A. Kuvshinov, L. Pesin, S. Chebotaryov et al., "Kinetics of radiation-induced carbonization of poly(vinylidene fluoride) film surface," *Polymer Degradation and Stability*, vol. 93, no. 10, pp. 1952–1955, 2008.

[52] I. V. Voinkova, N. N. Ginchitskii, I. V. Gribov et al., "A model of radiation-induced degradation of the poly(vinylidene fluoride) surface during XPS measurements," *Polymer Degradation and Stability*, vol. 89, no. 3, pp. 471–477, 2005.

[53] O. B. Hager, D. D. Gagliardi, and H. B. Walker, "Analysis of tear strength," *Textile Research Journal*, vol. 17, no. 7, pp. 376–381, 1947.

[54] Y. Lv, Y. Huang, M. Kong, Q. Yang, and G. Li, "Multivariate correlation analysis of outdoor weathering behavior of polypropylene under diverse climate scenarios," *Polymer Testing*, vol. 64, pp. 65–76, 2017.